Determination of the electronic state and concentration of nickel in NiSAPO catalysts by magnetic measurements

P. Dutta[a], A. Manivannan[a], M.S. Seehra[a,*], P.M. Adekkanattu[b], and J.A. Guin[b]

[a]*Department of Physics, West Virginia University, Morgantown WV 26506, USA*
[b]*Department of Chemical Engineering, Auburn University, Auburn AL 36849, USA*

Received 17 November 2003; accepted 19 February 2004

A method to determine the electronic state and concentration of Ni in Ni-loaded silicoaluminophosphate (NiSAPO-*n*) where *n* denotes the structure type ($n = 47$, 18, 34, 44, 56 and 17) is presented. The method involves measurements and analysis of the magnetization M versus magnetic field H (up to 55 kOe at 2 K) and M versus temperature ($T = 2$–300 K) data. The analysis yields spin $S = 1/2$ corresponding to Ni(I) state for lightly doped samples, whereas for higher doping, both Ni(I) and Ni(0) are indicated. The concentration of Ni determined from these studies varies between the minimum of 0.2 wt% for the $n = 47$ sample to maximum of 1.75% for the $n = 17$ sample.

KEY WORDS: SAPO-*n* molecular sieves; nickel species; magnetization; magnetic susceptibility.

Molecular sieve catalysts based on silicoaluminophosphate (SAPO-*n*) and aluminophosphate (AlPO-*n*) have been of considerable interest in recent years [1]. However, incorporation of transition metal ions such as Co, Ni, Mn etc. into the framework of SAPO-*n* in order to develop reaction-specific catalysts is not straightforward. So far, three different techniques *viz*. impregnation, ion-exchange, and the isomorphous substitution have been found successful for incorporating the transition metal ions [2]. Catalytic activity of the doped catalysts depends upon the valence state, location, dispersion and concentration of the metal species. Such information is often difficult to obtain when the concentration of the metal ion is less than 1%. The use of several techniques *viz*. electron magnetic resonance (EMR), electron spin echo modulation (ESEM) spectroscopy, and X-ray absorption fine structure (EXAFS) has been reported to characterized Ni in SAPO-*n* structures [3–5]. In this paper, we present the use of a different technique *viz*. magnetometry, to determine the concentration and electronic states and of Ni in SAPO-*n* catalysts which involves the analysis of the magnetization (M) data as a function of magnetic field H and temperature T. Details are given below.

SAPO and NiSAPO molecular sieves were synthesized by hydrothermal crystallization under autogeneous pressure using various organic templates. The following chemicals were used: orthophosphoric acid (85 wt%), aluminum isopropoxide (98 + %), pseudoboehmite (Catapal-B, 70 wt% Al_2O_3), fumed silica (99.8 wt%, 380 m^2/g), colloidal silica (Ludox LS, 30 wt%), nickel acetate tetra hydrate (99.98 wt%), cyclohexylamine (99 + wt%), *N*,*N*-diisopropylethylamine (99 wt%), morpholine (99 + wt%), tetraethylammonium hydroxide (30 wt% in water), methylbutylamine (96 wt%), *N*,*N*,*N*',*N*'-tetramethylhexane 1,6-diamine (99 wt%). All the chemicals except pseudoboehmite were from Aldrich. Pseudoboehmite was from Vista. Syntheses were carried out in a 120 cm^3 stainless steel autoclave lined with Teflon. Table 1 lists the molar compositions and crystallization conditions for the NiSAPO molecular sieves. The individual compositions and crystallization conditions were optimized by trial and error and based on literature reports on corresponding materials [1,6,7–15]. For brevity, we give below the detailed procedure for SAPO-17 and NiSAPO-17 only, with the other preparations being similar.

Cyclohexylamine was the organic template used for the synthesis of SAPO-17. In a typical synthesis 27.79 g aluminum isopropoxide was slurried in 45 g water and stirred for 30 min. Then 15.38 g phosphoric acid was added dropwise to this slurry followed by 20 g of water. The mixture was stirred for 2 h before adding 0.8 g of fumed silica and 4.7 g of water. The mixture was then stirred for 1 h before adding dropwise 6.68 g cyclohexylamine. The final mixture was stirred for 2 h to make the gel homogeneous. Then about 200 mg of $AlPO_4$-17 seed crystals were added to this gel and stirred for another 30 min. The pH of the gel was around 7.0. About 80 mL of the gel was loaded into a 120 mL autoclave and kept at 200 °C for 42 h. The product appeared as a fine powder and was separated from the mother liquor by centrifugation. It was then washed with water by repeated centrifugation, followed by drying at 70 °C overnight.

* To whom correspondence should be addressed.
E-mail: mseehra@wvu.edu

1011-372X/04/0500–0181/0 © 2004 Plenum Publishing Corporation

Table 1
Gel compositions and the crystallization conditions for NiSAPO-*n* molecular sieves

Structure	Template (R)	Molar gel composition	Temperature (°C)	Time (h)
NiSAPO-17	Cyclohexylamine	0.03NiO : 0.98 Al_2O_3 : 1.0 P_2O_5 : 0.1 SiO_2 : 1.0 R : 60 H_2O	200	42
NiSAPO-18	*N*,*N*-diisopropyl-ethylamine	0.03NiO : 0.98 Al_2O_3 : 0.92 P_2O_5 : 0.3 SiO_2 : 1.6 R:50H_2O	165	184
NiSAPO-34	Morpholine	0.03NiO : 0.98 Al_2O_3 : 1.0 P_2O_5 : 0.6 SiO_2 : 2.0 R : 60 H_2O	200	49
NiSAPO-44	Cyclohexylamine	0.03NiO : 0.98 Al_2O_3 : 1.0 P_2O_5 : 0.6 SiO_2 : 1.9 R : 60 H_2O	190	48
NiSAPO-47	Methylbutylamine	0.03NiO : 0.98 Al_2O_3 : 1.0 P_2O_5 : 0.3 SiO_2 : 2.0 R : 60 H_2O	200	110
NiSAPO-56	*N*,*N*,*N*′,*N*′,-tetramethyl-hexane 1,6 diamine	0.03NiO : 1.0 Al_2O_3 : 1.0 P_2O_5 : 0.3 SiO_2 : 1.0 R : 40 H_2O	200	111

Synthesis of the NiSAPO-17 was achieved by following the same procedure except that nickel acetate was first mixed with the phosphoric acid and the resulting solution was added to the alumina slurry. Product recovery was same as SAPO-17.

All the SAPO materials in their as-synthesized form contain organic templates occluded in the channels and cages. The organic templates were removed by slowly heating to 550 °C in air and kept at this temperature for 12 h. This calcination process effectively converts the SAPO materials into their corresponding H-SAPO form. Based on the Ni content in the gel mixtures in table 1, the wt% Ni in the calcined catalysts would have an expected nominal value of around 0.7 wt%.

The magnetic data are presented on six different structure types for $n = 17$, 18, 34, 44, 47 and 56. All the samples were characterized and identified to be pure SAPO phases by room temperature X-ray diffraction (XRD) using a Rigaku diffractometer with CuK_α radiation. However, XRD did not provide any information on Ni -loading partly because of low levels of Ni loading. Measurements of the magnetization M as a function of temperature ($T = 2$–300 K) and magnetic field H up to 55 kOe were carried out on a commercial superconducting quantum interference device (SQUID) magnetometer. The samples were tightly packed into a white plastic drinking straw as the sample holder. The data presented here are corrected for the background diamagnetic susceptibility of the sample holder, which is independent of T and H and has the magnitude $\chi = -3\times10^{-8}$ emu/Oe.

Two sets of data are reported here: First, the variation of M with H at the lowest experimental $T = 2$ K with H up to 55 kOe and second the variation of M versus T from 2–300 K at a fixed $H = 100$ Oe. The variations of M versus H at 2 K for the six samples are shown in figure 1. For a paramagnet with unpaired spin S, the variation of M versus H is expected to follow the Brillouin function $B_s(x)$ given by [16]

$$\frac{M}{M_0} = B_s(x) = \frac{2S+1}{2S}\coth\left(\frac{2S+1}{2S}x\right) - \frac{1}{2S}\coth\left(\frac{x}{2S}\right) \quad (1)$$

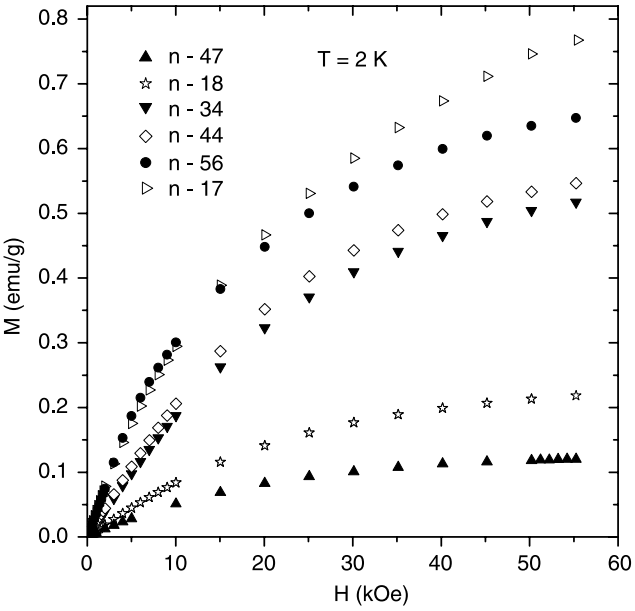

Figure 1. Plots of the magnetization M versus field H at $T = 2$ K for all samples.

where $x = g\mu_B SH/k_B T$, with μ_B being the Bohr magneton, k_B the Boltzmann constant and g the g-value of the paramagnetic ion. In equation (1), M_0 is the saturation magnetization which can be estimated from the value of M in the limit $1/H \to 0$.

Theoretically, M_0 is given by [16]

$$M_0 = Ng\mu_B S \quad (2)$$

with N being the concentration of paramagnetic ions. The fitting of the data of figure 1 to equations (1) and (2) can in principle determine both S and N. Fits to equation (1) for four samples are shown in figure 2 and the remaining two samples in figure 3 with magnitudes of M_0 and N given in table 2. In the figures 2 and 3, we have also shown the theoretical curves for $B_S(x)$ for $S = 1/2$, 1 and 3/2 . The data for the samples with structure type $n = 18$, 34, 44, and 47 fits very well with $S = 1/2$ in figure 2, whereas in figure 3 theoretical fits for the samples with $n = 17$ and 56 with any S value is quite poor. As we shall see later, for these two samples, some of the Ni is precipitated out as Ni(0) nanoparticles

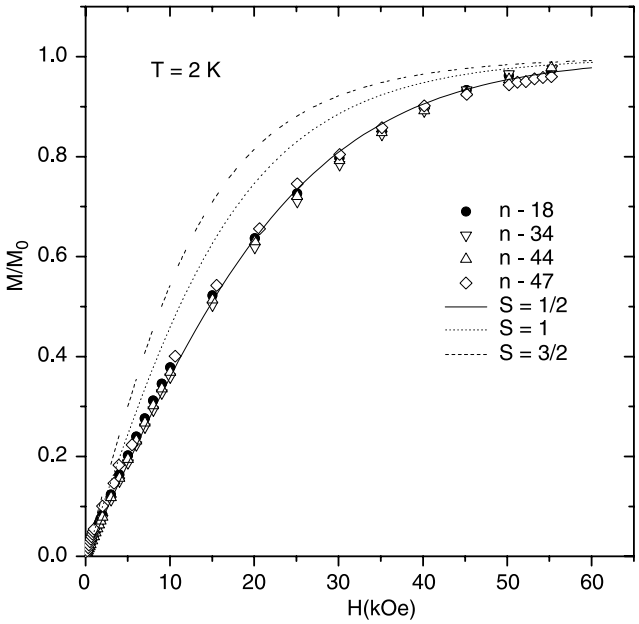

Figure 2. Plots of the normalized magnetization M/M_0 against H at 2 K for the samples NiSAPO-18, NiSAPO-34, NiSAPO-44, NiSAPO-47. The theoretical curves are equation (1) for spin 1/2, 1, 3/2.

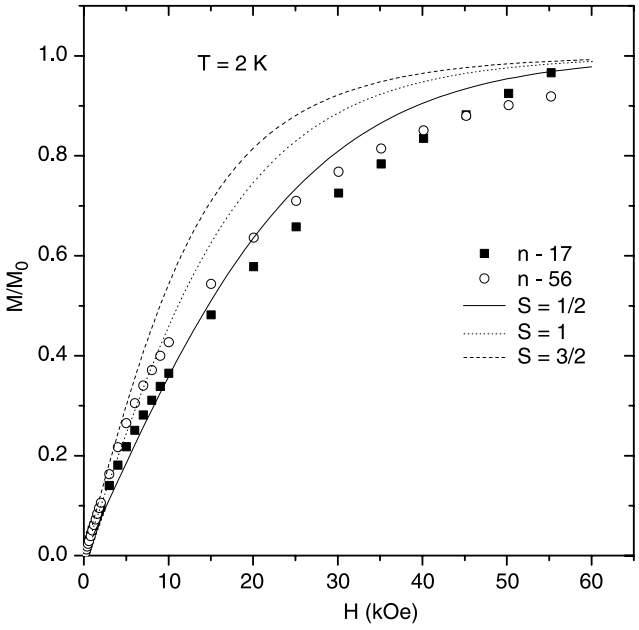

Figure 3. Same plots as figure 2 for the samples NiSAPO-17, NiSAPO-56.

making the fitting to $B_S(x)$ quite questionable. Also, because of the small magnitude of $gS = 0.6$ for Ni(0) state, the experimental values of M/M_0 even lower than the predicted $S = 1/2$ is quite understandable.

To determine the concentration of N of paramagnetic spins using equation (2), we use g = 2.23 for Ni ions and $S = 1/2$ determined above. This yields wt% Ni = 0.942 M_0 using the molecular weight of SAPO as 122. In table 2, we list the wt% Ni so calculated for the six samples. These results are discussed later.

A second procedure for the calculation of N is possible by fitting the magnetic susceptibility (χ) data against T to the Curie–Weiss law:

$$\chi = \chi_0 + \frac{C}{T - \theta} \tag{3}$$

where χ_0 is the high temperature χ in the limit $1/T \to 0$ and includes contribution from the host SAPO-n and van Vleck contribution from the Nickel ions [17]. The magnitudes of χ_0 was determined by plotting χ versus $1/T$ and taking the limit $1/T \to 0$. These magnitudes are listed in table 2. To determine the Curie constant C and the Weiss temperature θ, $1/(\chi - \chi_0)$ is then plotted against T, the slope yields $1/C$ and the intercept θ. The magnitudes of C and θ are also listed in table 2. The results of these fits are shown in figure 4 and figure 5 in the plots of χ versus T on a semilog scale in order to detail the behavior at lower T. For the four samples with $n = 18$, 34, 47 and 48, the data fit equation (3) quite well, whereas for the other two samples in figure 5, the data show a peak in χ near $T_B = 5$ K below which the data for the zero-field cooled (ZFC) and the field-cooled (FC) cases bifurcate. This bifurcation below the blocking temperature T_B is characteristic of nanoparticle magnetism [18] as we will discuss later. However for $T > T_B$, the data can be fitted to equation (3) quite well and the constants C and θ are also listed in table 2.

The Curie constant is $C = N g^2 \mu_B{}^2 S(S+1)/3k_B$ [16]. Again using $g = 2.23$ and $S = 1/2$, the wt% of Ni is calculated to $= 1.257 \times 10^4$ C. The results of these calculations are also listed in table 2. The Weiss-temperature θ is a measure of exchange interaction between paramagnetic spins; a positive (negative) θ represents ferromagnetic (antiferromagnetic) interaction. The small magnitudes of θ indicate weak interaction because of low loadings of Ni.

Table 2
Experimental parameters for all six NiSAPO samples

Structure	χ_0 (10^{-7}) emu/g Oe	C (10^{-5}) emu K/g Oe	θ (K)	Ni wt% calculated from C	M_0 (emu/g)	Ni wt% calculated from M_0	Ni-nano particles
NiSAPO-18	6.3	2.0	0	0.25%	0.2215	0.21%	No
NiSAPO-34	9.3	6.0	− 2	0.75%	0.5414	0.51%	No
NiSAPO-44	4.6	6.1	0	0.77%	0.5585	0.53%	No
NiSAPO-47	18.6	1.5	− 1	0.19%	0.1218	0.11%	No
NiSAPO-56	6.4	8.9	+4	1.11%	0.7321	0.69%	Yes
NiSAPO-17	5.2	14.0	+4	1.75%	0.9125	0.86%	Yes

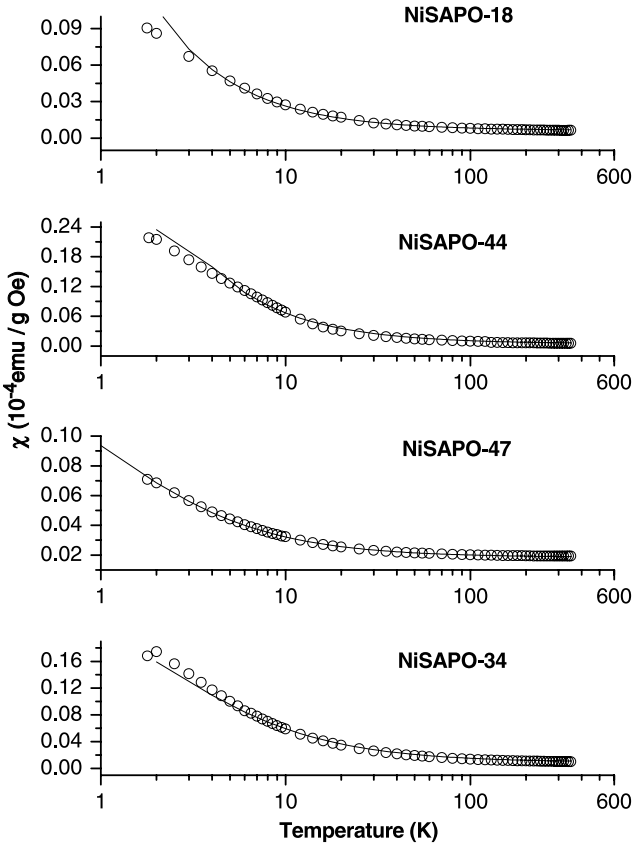

Figure 4. Temperature variation of the magnetic susceptibility $\chi = M/H$ at $H = 100$ Oe for the samples NiSAPO-18, NiSAPO-34, NiSAPO-44, NiSAPO-47. The solid lines are fit to the Curie-Weiss law (equation (3)) with fitting parameters shown in table 2.

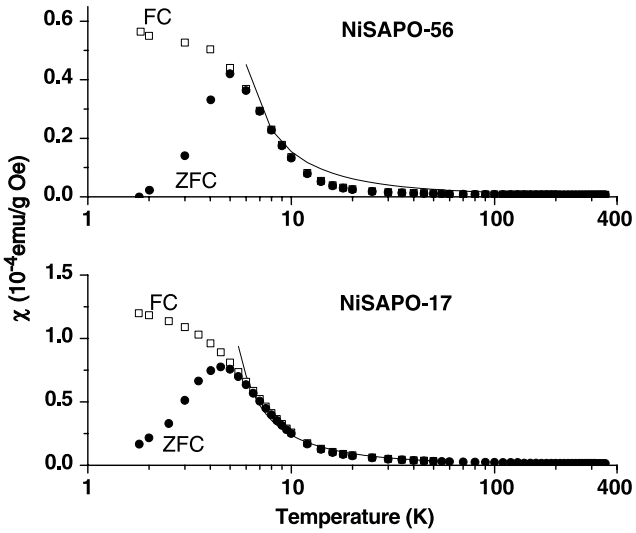

Figure 5. Temperature dependence of χ for the ZFC and the field cooled (FC) cases for samples NiSAPO-17, NiSAPO-56. The solid lines are fits to equation (3) for $T > T_B = 5$ K, with parameters given in table 2.

An examination of the wt% Ni in table 2, calculated by the two methods shows that the magnitudes calculated from C tend to be higher by as much as 50% compared to those calculated from M_0. This is not yet completely understood. The other issue requiring discussion is the magnitude of $S = 1/2$ determined from the fit to equation (1) in figure 2. For Ni(II) such as in NiO, $S = 1$ is expected, although because of large zero-point spin deviations, the measured experimental value of $S = 0.8$ [17]. On the other hand, for Ni(I), $S = 1/2$ is the expected value [16], indicating that at least for NiSAPO-n with $n = 18$, 34, 44, and 47, Ni(I) electronic state is present. For the other two samples with $n = 17$ and 56 where T_B is observed, at least part of the Ni is in the Ni(0) state. Azuma and Kevan [4] have reported detailed studies of the ESR sensitive nickel-based species in SAPO samples. These studies show that Ni(II) in SAPO is ESR silent, Ni(I) species are observed only after prolonged dehydration of the samples at higher temperatures with $g = 2.22$ and Ni(0) gives a very broad signal. We checked for ESR signals at 9.28 GHz in the samples of table 2 at temperatures down to 5 K, but without evacuation or thermal treatment of the samples. No signal could be observed. The absence of ESR signal in our experiments is however completely consistent with the presence of Ni(I) and Ni(0) states as discussed above.

In summary, the results presented here have shown that analysis of M versus H and M versus T data in NiSAPO-n samples yield the electronic state of Ni as Ni(I) for light doping and Ni(I) and Ni(0) for higher dopings. This analysis is useful even when the concentrations of Ni are ≤1%. Similar analysis should be equally effective for other paramagnetic ions (e.g. Mn, Fe, Co and Cu). However, if more than one paramagnetic ion is present in a sample, the analysis will be more difficult because M measures the effects of all magnetic species in a sample.

Acknowledgments

This work was supported by the U.S. Department of Energy, Contract No. DE-FC26-02NT41594, through the Consortium for Fossil Fuel Science.

References

[1] J.M. Thomas, Angew. Chem., Int. Ed. Engl. 27 (1988) 1673.
[2] M. Hartmann and L. Kevan, Chem. Rev. 99 (1999) 635.
[3] A.M. Prakash, T. Wasowicz and L. Kevan, J. Phys. Chem. 100 (1996) 15947.
[4] N. Azuma and L. Kevan, J. Phys. Chem. 99 (1995) 5083.
[5] M. Sano, T. Maruo, H. Yamatera, M. Sujuki, and Y. Saito, J. Am. Chem. Soc. 52 (1987) 109.
[6] D.R. Dubois, D.L. Obrzut, J. Liu, J. Thundimadathil, P.M. Adekkanattu, J.A. Guin, A. Punnoose and M.S. Seehra, Fuel. Proc. Tech. 83 (2003) 203.
[7] J. Chen, P.A. Wright, J.M. Thomas, S. Natarajan, L. Marchese, S.M. Bradley, G. Sankar, C.R.A. Catlow, P.L. Gai-Boyes, R.P. Townsend and C.M. Lok, J. Phys. Chem. 98 (1994) 10216.
[8] M.A. Djieugoue, A.M. Prakash and L. Kevan, J. Phys. Chem. B. 104 (2000) 6452.

[9] A.M. Prakash and L. Kevan, Langmuir 13 (1997) 3341.
[10] B.M. Lok, C.A. Messina, R.L. Patton, R.T. Gajek, T.R. Cannan and E.M. Flanigen, US Pat. 4,440,871 (1984)
[11] A.M. Prakash and S. Unnikrishnan, J. Chem. Soc. Faraday Trans. 90 (1994) 2291.
[12] S. Ashtekar, S.V.V. Chilukuri and D.K. Chakrabarty, J. Phys. Chem. 98 (1994) 4878.
[13] A.M. Prakash, S. Unnikrishnan and K.V. Rao, *Applied Catalysis A* Vol. 110 (Elsevier, Amsterdam 1994), p.1.
[14] E. Dumitriu, D. Lutic, V. Hulea, D. Dorohoi, A. Azzouz, E. Colnay and C. Kappenstein, Micropor. Mesopor. Mater. 31 (1999) 187.
[15] S.T. Wilson, U.S. Patent 5 370 851 (1994).
[16] C. Kittel, *Introduction to Solid State Physics*, 7th ed. (Wiley, New York, 1996) pp. 417–484.
[17] G. Srinivasan and M.S. Seehra, Phys. Rev. B 29 (1984) 6295.
[18] M.S. Seehra, V.S. Babu, A. Manivannan and J.W. Lynn, Phys. Rev. B. 61 (2000) 3513.